L-Dopa induced dyskinesias require Cholinergic Interneuron expression of Dopamine 2 receptor.

Santiago Uribe-Cano, MA,[1,2] Lauren Malave, PhD,[3] Andreas H. Kottmann, PhD[1,2,4]

[1]Department of Molecular, Cellular and Biomedical Sciences, CUNY School of Medicine at City College of New York, City University of New York, New York, NY, USA

[2]City University of New York Graduate Center, Neuroscience Collaborative, New York, NY, USA

[3]Department of Psychiatry, Columbia University, New York, NY, USA

[4]City University of New York Graduate Center, Molecular, Cellular and Developmental Subprogram, New York, NY, USA

Correspondence to: Dr. Andreas H. Kottmann, Dept. of Molecular, Cellular and Biomedical Research
CUNY School of Medicine at City College of New York Center for Discovery and Innovation
85 St. Nicholas Terrace; 3-314, New York City, NY 10031; E-mail: AKottmann@med.cuny.edu

Word Counts: Abstract – 137; Main Text – 1606

Running title: L-Dopa induced dyskinesias require CIN D2

Key Words: Cholinergic Interneurons, Dopamine 2 Receptor, L-Dopa, Dyskinesias, Parkinson Disease,

ABSTRACT:

Background: Striatal Cholinergic Interneurons (CIN) are drivers of L-Dopa induced Dyskinesias (LID). However, what signaling pathways elicit aberrant CIN activity remains unclear. CIN express D2 and D5 receptors suggesting repeated activation of these receptors in response to L-Dopa could promote LID. While the role of D5 in this process has recently been probed, little is known about the role of D2.

Method: Mice with CIN-specific D2 ablation ($D2_{CIN}KO$) underwent unilateral 6-OHDA lesion and chronic L-Dopa dosing, throughout which LID severity was quantified. The effect of $D2_{CIN}KO$ on histological markers of LID severity and CIN activity were also quantified postmortem.

Results: $D2_{CIN}KO$ attenuated LID across L-Dopa doses, reduced expression of histological LID marker p-ERK, and prevented L-Dopa-induced increases in CIN activity marker p-rpS6 in the dorsolateral striatum.

Conclusion: The activation of D2 specifically on CIN is a key driver of LID.

Introduction

Dopamine (DA) supplementation via L-Dopa is initially effective at attenuating akinesia among Parkinson's patients but progressively diminishes in efficacy and eventually induces debilitating dyskinesias.[1] Recent work indicates that these L-Dopa Induced Dyskinesias (LIDs) are caused by maladaptive DA plasticity in the Striatum which normally facilitates motor learning.[2]

From a circuit standpoint, Dopamine 1 receptor (D1) and Dopamine 2 receptor (D2) expressing medium spiny neurons (MSN) as well as Cholinergic Interneurons (CIN), which regulate MSN, have been implicated in LID.[3–5] The regulation of MSN by CIN concurs with evidence that inhibition or ablation of CIN attenuates LID and suggests CIN are drivers of LID.[6] Normalizing CIN physiology in the Parkinsonian brain thus offers a powerful approach by which to preserve L-Dopa benefits while curtailing LID-promoting effects.

CIN integrate many GPCR pathways, several of which appear to modulate LID.[7–9] Among these, Gi-coupled D2 and Gs-coupled D5 are of particular interest given L-Dopa increases DA and these receptors represent a direct route by which L-Dopa might disrupt CIN physiology and promote LID. While the role of D5 in this process has recently been investigated,[8,10] the role of CIN D2 in LID has received little attention. This is in part due to difficulty separating manipulations of D2 on CIN from D2 on MSN. To overcome this, we combined selective Cre-Lox ablation of D2 from CIN with the unilateral 6-OHDA mouse model of LID. We find that ablation of D2 from CIN attenuates LID, prevents changes in CIN activity, and blocks activation of LID-associated marker p-ERK.

Materials and Methods

70 **Animals:** Heterozygous $D2^{L/+}$:$ChATCre^{+/-}$ animals served as controls. Homozygous $D2^{L/L-}$
71 :$ChATCre^{+/-}$ animals provided CIN-specific ablation of D2 ($D2_{CIN}$ KO).[11] Recombination of the
72 D2 allele was detected in striatal tissue but was absent in tail tissue (FIG 1. A).

73 **6-OHDA Lesion and L-Dopa Treatment**: Animals received unilateral 6-OHDA in the DL
74 striatum. Parkinsonian phenotype was assessed after 3 weeks via turn bias in the open field and
75 ipsilateral paw-use bias in the cylinder test as previously described.[9] Animals received daily L-
76 Dopa (5–20Mg/Kg) and benserazide in saline. Therapeutic L-Dopa effects in open field and
77 cylinder tests were quantified after the first dose as previously detailed.[9] Daily L-Dopa was
78 administered at 5Mg/Kg (Day 1-13), 10Mg/Kg (Day 14-16), 15Mg/Kg (Day 17-18), and 20Mg/Kg
79 (Day 19-31) with total abnormal involuntary movements (a validated measure of dyskinesia;
80 AIMs) regularly quantified as outlined previously.[9] Upon completion of the full 31-day dosing
81 schedule, half the animals underwent 1 week L-Dopa washout (saline only) while the other half
82 continued L-Dopa exposure at 20Mg/Kg. Thirty minutes after the final L-Dopa or saline dose,
83 animals were sacrificed and tissue processed for immunohistochemistry.

84 **Immunohistochemistry:** Antibodies can be found in [9]. Fluorescence from confocal images was
85 quantified via ImageJ. To assess DA neuron (DAN) loss in the striatum Tyrosine Hydroxylase
86 Mean Gray Value (MGV) was calculated for ROIs covering the DL striatum and normalized by
87 background MGV. Average fold-change between 6-OHDA and non-treated hemispheres was
88 calculated for each animal. For detection of p-ERK^+ CIN, we identified CIN ROIs ($ChAT^+$ cells)
89 and p-ERK MGV was measured in CIN of the lesioned and unlesioned hemispheres. Average and
90 standard deviation of CIN-specific p-ERK values was calculated for unlesioned hemispheres of
91 each animal. Lesioned hemisphere CIN were considered p-ERK^+ if their MGV was greater than
92 the average plus 2StdDev of the unlesioned hemisphere. Total percent of p-ERK^+ CIN was

93 reported for each lesioned striatum. The same procedure was utilized to detect p-ERK$^+$ NeuN$^+$
94 cells, with the exception that ROIs were formed around NeuN$^+$/ChAT$^-$ cells. For analysis of
95 ribosomal protein S6 phosphorylation (p-rpS6), MGV was calculated for ChAT ROIs and
96 normalized by background MGV.

97 **Results**

98 **Loss of D2 Signaling on CIN Attenuates L-Dopa Induced Dyskinesias**

99 Heterozygous controls and D2$_{CIN}$KO animals showed similar striatal DAN degeneration
100 following 6-OHDA (FIG 1. A, B). Both also showed equivalent ipsilateral turn-bias in the open
101 field (FIG.1 C) and predominant use of ipsilateral paw in the cylinder test (FIG 1. D). Subsequent
102 administration of L-Dopa at 5Mg/Kg reversed turn-bias in the open field and promoted equal use
103 of ipsilateral and contralateral paws in the cylinder test equivalently among controls and D2$_{CIN}$ KO
104 animals (FIG 1. C, D). These data suggest that selective ablation of D2 from CIN does not reduce
105 6-OHDA cyto-toxicity nor anti-akinetic L-Dopa effects.

106 Control animals showed sustained AIMs throughout treatment that increased in severity as
107 L-Dopa dose escalated on days 14, 17, and 19 (FIG 1. E). In contrast, D2$_{CIN}$KO animals showed
108 attenuated AIMs across L-Dopa treatment. AIM subtypes reflected this absence of total AIMs
109 among D2$_{CIN}$KO animals with attenuated expression across axial, limb, and orofacial AIMs (FIG
110 1. G). Fitting total AIM severity across each of the four L-Dopa doses tested using simple linear
111 regression further supported the absence of LID escalation among D2$_{CIN}$KO (FIG 1. F). The
112 resulting slopes for each genotype showed significant difference suggesting the positive
113 relationship between L-Dopa dose and AIM severity observed in controls was absent among

114 $D2_{CIN}KO$ animals. Therefore, the absence of D2 on CIN not only attenuates LID, but also disrupts
115 the dose-dependency of LID severity.

116 **LID Marker p-ERK Reflects Attenuation of AIMs in $D2_{CIN}KO$ Animals**

117 Phosphorylation of extracellular signal-regulated kinase1/2 (p-ERK) in the
118 hypodopaminergic striatum reflects both LID severity and time-course.[9,12] Specifically, early-
119 stage L-Dopa treatment promotes p-ERK expression among MSNs while chronic treatment shifts
120 p-ERK expression from MSNs to CIN.[12] Given the chronic nature of our L-Dopa treatment, we
121 examined CIN p-ERK expression in controls and $D2_{CIN}KO$ animals to see if the attenuation of LID
122 observed among $D2_{CIN}KO$ animals was reflected by changes in CIN p-ERK.

123 In accordance with behavioral observations (Fig. 1 E), we found ~6-fold reduction in p-
124 ERK^+ CIN of the DL striatum among $D2_{CIN}KO$ animals compared to controls (FIG 2. A, B). The
125 percentage of p-ERK^+ CIN in the DM striatum however was similarly low in $D2_{CIN}KO$ and control
126 animals when compared to the control DL striatum, a finding in accordance with the predominant
127 role of the DL striatum in LID. Further, p-ERK levels in non-cholinergic, $NeuN^+$ neurons of the
128 striatum were not affected by $D2_{CIN}KO$ (FIG 2. C). Together, this confirms that CIN-specific
129 differences in LID-associated p-ERK reflect the attenuation of LID observed in $D2_{CIN}KO$ animals
130 (Won, Ding et al. 2014) and suggests that D2 activation is required for CIN expression of p-ERK.

131 **$D2_{CIN}KO$ prevents L-Dopa Induced Increases in CIN-specific p-rpS6**

132 To investigate whether D2 contributes to changes in CIN activity following L-Dopa we
133 quantified levels of p-rpS6, a marker of CIN activity.[13] Specifically, we aimed to isolate the
134 effect of $D2_{CIN}$ on activity after LID has been established as opposed to the preceding long-term
135 changes chronic L-Dopa likely produces. We therefore compared DL CIN in 6-OHDA treated

136 control and $D2_{CIN}KO$ animals that underwent normal L-Dopa treatment (L-Dopa ON) or a washout
137 period after treatment (L-Dopa OFF) prior to analysis.

138 Comparison of CIN p-rpS6 in unlesioned hemispheres of L-Dopa OFF control and
139 $D2_{CIN}KO$ animals showed no difference, suggesting no baseline effect of $D2_{CIN}KO$ in the intact
140 DL striatum (FIG 2. E). Similarly, we found $D2_{CIN}KO$ did not impact CIN activity in 6-OHDA
141 lesioned hemispheres of L-Dopa OFF animals (FIG 2. F column 1 vs column 3). However, when
142 we examined the effects of $D2_{CIN}KO$ on p-rpS6 levels in 6-OHDA lesioned hemispheres of L-
143 Dopa ON animals, L-Dopa treatment altered CIN p-rpS6 levels in control but not $D2_{CIN}KO$
144 animals (FIG 2. F) suggesting that $D2_{CIN}$ in the hypodopaminergic brain modifies CIN activity in
145 response to L-Dopa. Unexpectedly, this effect was excitatory, in apparent violation of a predicted
146 Gi-mediated CIN inhibition by D2. Anatomically, this change in activity was mediated by
147 dorsolateral-most CIN. Linear regression fitting each CIN's p-rpS6 value and distance from the
148 DL apex of the striatum revealed that while CIN activity was relatively equal across the striatum
149 of control 6-OHDA animals in the L-Dopa OFF state (FIG 2. G; Gray), the addition of L-Dopa
150 promoted activity in dorsolateral-most CIN (FIG 2. G; Comparison of Gray vs Green Slopes). In
151 contrast, L-Dopa exposure had little effect on the p-rpS6 levels of dorsolateral-most CIN in
152 $D2_{CIN}KO$ animals (FIG 2. G; Red vs Brown). These data reveal that L-Dopa exposure after a
153 schedule of chronic treatment promotes CIN activity in the DL striatum. Paradoxically however,
154 we find that $D2_{CIN}KO$ attenuates this excitation and simultaneously attenuates CIN p-ERK levels
155 and AIM severity.

156 **Discussion**

157 Here we find that repeated L-Dopa treatment after 6-OHDA lesioning does not produce
158 LID in mice with selective $D2_{CIN}KO$. Our results support prior observations that LID is

159 characterized by elevated CIN activity and that their ablation or inhibition prevents LID.[6,12,14]
160 However, these studies left unanswered which signaling pathway(s) on CIN induce their aberrant
161 and LID promoting activity. The results presented here highlight $D2_{CIN}$ as an unexpected and
162 critical component of LID-associated CIN hyperactivity (p-rpS6) and MAP kinase pathway
163 activation (p-ERK).

164 So called "paradoxical", i.e. facilitatory responses to $D2_{CIN}$ activation have been previously
165 described in the literature: Quinpirole activation of $D2_{CIN}$ in a mutant TorsinA mouse model results
166 in elevated CIN firing compared to controls.[15] Changes in the coupling efficiency between
167 D2/Gi and D2/B-arrestin have also been suggested to modify the effect of D2 activation.[15,16]
168 Additionally, inhibition of the integrated stress response in CIN similarly seems to switch D2 from
169 inhibitory to facilitatory.[17] These observations along with our own conform with the finding that
170 ablation of DAN decreases the excitability of CIN despite a simultaneous reduction of supposedly
171 inhibitory D2 activation.[14,18,19] Thus, it becomes possible that changes in the Parkinsonian
172 brain activate mechanisms by which the downstream action of $D2_{CIN}$ is modified, resulting in CIN
173 hyperexcitability and LID development. Understanding in molecular detail the processes
174 underlying these changes might open new avenues to counter maladaptive plasticity among CIN
175 in PD, LID, and beyond.

176 **Acknowledgments:** We thank A. Walls for helpful discussion and technical assistance with PCR
177 assays. We also thank K. Liu for assistance with tissue preparation, staining, and data collection.

178

Author Roles:

1. Research project: A. Conception, B. Organization, C. Execution;
2. Statistical Analysis: A. Design, B. Execution, C. Review and Critique;
3. Manuscript Preparation: A. Writing of the first draft, B. Review and Critique;

Santiago Uribe-Cano: 1B, 1C, 2A, 2B, 3A, 3B,

Lauren Malave: 1A, 2C, 3B

Andreas H Kottmann: 1A, 1B, 2C, 3A, 3B

All authors had final approval of the submitted version

Disclosures:

Relevant Conflicts of Interest/Financial Disclosures: Nothing to Report

Funding Sources: This study was supported by National Institute of General Medical Sciences (NIGMS; T32GM136499), National Institute on Aging (NIA; AG065682), National Institute for Neurological Diseases and Stroke (NINDS; NS095253) and the American Parkinson's Disease Association (APDA).

Ethical Compliance Statement:

- All mouse experiments were approved by the IACUC committee of City College of New York.

198 **References**

199 1 Bastide MF, Meissner WG, Picconi B, *et al.* Pathophysiology of L-dopa-induced motor
200 and non-motor complications in Parkinson's disease. *Progress in Neurobiology*.
201 2015;132:96–168.

202 2 Cheung THC, Ding Y, Zhuang X, *et al.* Learning critically drives parkinsonian motor
203 deficits through imbalanced striatal pathway recruitment. *Proceedings of the National*
204 *Academy of Sciences*. 2023;120:e2213093120.

205 3 Picconi B, Centonze D, Håkansson K, *et al.* Loss of bidirectional striatal synaptic
206 plasticity in L-DOPA–induced dyskinesia. *Nature Neuroscience*. 2003;6:501–6. doi:
207 10.1038/nn1040

208 4 Shen W, Flajolet M, Greengard P, *et al.* Dichotomous Dopaminergic Control of Striatal
209 Synaptic Plasticity. *Science*. 2008;321:848–51.

210 5 Aldrin-Kirk P, Heuer A, Rylander Ottosson D, *et al.* Chemogenetic modulation of
211 cholinergic interneurons reveals their regulating role on the direct and indirect output
212 pathways from the striatum. *Neurobiology of Disease*. 2018;109:148–62.

213 6 Won L, Ding Y, Singh P, *et al.* Striatal Cholinergic Cell Ablation Attenuates l-DOPA
214 Induced Dyskinesia in Parkinsonian Mice. *J Neurosci*. 2014;34:3090–4.

215 7 Lim SAO, Kang UJ, McGehee DS. Striatal cholinergic interneuron regulation and circuit
216 effects. *Front Synaptic Neurosci*. 2014;6. doi: 10.3389/fnsyn.2014.00022

217 8 Cortés M, Malave L, Castello J, *et al.* CK2 Oppositely Modulates l-DOPA-Induced
218 Dyskinesia via Striatal Projection Neurons Expressing D1 or D2 Receptors. *J Neurosci*.
219 2017;37:11930–46.

220 9 Malave L, Zuelke DR, Uribe-Cano S, *et al.* Dopaminergic co-transmission with sonic
221 hedgehog inhibits abnormal involuntary movements in models of Parkinson's disease and
222 L-Dopa induced dyskinesia. *Commun Biol*. 2021;4:1–16.

223 10 Paz RM, Stahl AM, Rela L, *et al.* D1/D5 Inverse Agonists Restore Striatal Cholinergic
224 Interneuron Physiology in Dyskinetic Mice. *Movement Disorders*. 2022;37:1693–706.

225 11 Bello EP, Mateo Y, Gelman DM, *et al.* Cocaine supersensitivity and enhanced motivation
226 for reward in mice lacking dopamine D2 autoreceptors. *Nat Neurosci*. 2011;14:1033–8.
227 doi: 10.1038/nn.2862

228 12 Ding Y, Won L, Britt JP, *et al.* Enhanced striatal cholinergic neuronal activity mediates l-
229 DOPA–induced dyskinesia in parkinsonian mice. *PNAS*. 2011;108:840–5.

230 13 Bertran-Gonzalez J, Chieng BC, Laurent V, *et al.* Striatal Cholinergic Interneurons
231 Display Activity-Related Phosphorylation of Ribosomal Protein S6. *PLOS ONE*.
232 2012;7:e53195.

233 14 Choi SJ, Ma TC, Ding Y, *et al.* Alterations in the intrinsic properties of striatal
234 cholinergic interneurons after dopamine lesion and chronic L-DOPA. *eLife*.
235 2020;9:e56920.

236 15 Scarduzio M, Zimmerman CN, Jaunarajs KL, *et al.* Strength of cholinergic tone dictates
237 the polarity of dopamine D2 receptor modulation of striatal cholinergic interneuron
238 excitability in DYT1 dystonia. *Experimental Neurology*. 2017;295:162–75.

239 16 Pisani A, Martella G, Tscherter A, *et al.* Altered responses to dopaminergic D2 receptor
240 activation and N-type calcium currents in striatal cholinergic interneurons in a mouse
241 model of DYT1 dystonia. *Neurobiology of Disease*. 2006;24:318–25.

242 17 Helseth AR, Hernandez-Martinez R, Hall VL, *et al.* Cholinergic neurons constitutively
243 engage the ISR for dopamine modulation and skill learning in mice. *Science*. 2021;372.
244 doi: 10.1126/science.abe1931

245 18 Maurice N, Mercer J, Chan CS, *et al.* D2 Dopamine Receptor-Mediated Modulation of
246 Voltage-Dependent Na+ Channels Reduces Autonomous Activity in Striatal Cholinergic
247 Interneurons. *J Neurosci*. 2004;24:10289–301.

248 19 McKinley JW, Shi Z, Kawikova I, *et al.* Dopamine Deficiency Reduces Striatal
249 Cholinergic Interneuron Function in Models of Parkinson's Disease. *Neuron*.
250 2019;103:1056-1072.e6.

251

252 **Figure Legends:**

253

254 **FIG 1. (A)** PCR validation of ChATCre-dependent D2 allele recombination. Primers produced
255 bands spanning exon 2 of the D2 allele and flanking Lox sites. Absence of recombined band in
256 tail samples suggests ChATCre-specific recombination in CIN of striatum. **(B)** Representative
257 image showing reduction of TH in the DL striatum following 6-OHDA. **(C)** Comparison of
258 quantified TH reduction in 6-OHDA hemisphere (Lesioned/Unlesioned) between controls and
259 $D2_{CIN}$ KO animals. (n = 5-7; unpaired two-tailed Student's t test $p = 0.79$ Control vs. $D2_{CIN}$ KO).
260 **(D)** Changes in turn bias (Contra/Ipsi turn ratio) produced by unilateral 6-OHDA and subsequent
261 treatment with L-Dopa 5Mg/Kg. Turn bias is reported as fold change from baseline in the open
262 field. (n = 5-7 per genotype; Matched Mixed-effects model; Timepoint effect: $F [1.002,$
263 $9.516] = 15.07$, $p = 0.0033$; Genotype effect: $F [1, 10] = 0.93$, $p = 0.36$. Post hoc Tukey's multiple
264 comparisons test: $^{**}p < 0.01$). **(E)** Changes in contralateral paw use among unilateral 6-OHDA
265 animals before and after L-Dopa. Percent of total rears favoring the paw contralateral to 6-
266 OHDA hemisphere is reported. (n = 5-7 per genotype; Two-way RM ANOVA; Timepoint effect:
267 $F [1, 10] = 20.67$, $p = 0.0011$; Genotype effect: $F [1, 10] = 0.21$, $p = 0.66$). **(F)** Total AIM scores
268 across the first 19 days of L-Dopa treatment. Day of treatment and L-Dopa dose are listed across
269 the X-axis. (n = 5-7 per genotype; Two-way RM ANOVA; Day/Dose effect: $F [2.462,$
270 $24.62] = 11.29$, $p = 0.0002$; Genotype effect: $F [1, 10] = 6.03$, $p = 0.034$; Genotype X Day/Dose
271 interaction: $F [5, 50] = 4.50$, $p = 0.0018$. Post hoc Tukey's multiple comparisons test: $^{*}p < 0.05$,
272 $^{**}p < 0.01$, $^{***}p < 0.001$). **(G)** Breakdown of AIM subtypes across days of L-Dopa treatment.
273 Average group value of AIM subtypes is reported in stacked bars. Column background indicates
274 genotype. **(H)** AIM severity plotted across L-Dopa doses for each genotype. Statistically

275 significant differences in the slope of the two lines was tested (n = 5-7 per genotype; ANCOVA:
276 F [1, 4] = 15.97, p = 0.0162).

277

278 **FIG 2. (A)** Quantification of p-ERK^{+} CIN reported as percent of total CIN in the DM or DL
279 striatum. (n = 6-8 Striata per genotype; Two-way RM ANOVA; Striatal Region effect: F [1,
280 12] = 5.96, p = 0.0311. Post hoc Šídák's multiple comparisons test: **p < 0.01). **(B)**
281 Representative images of p-ERK and ChAT expression in the DL striatum. **(C)** Quantification of
282 p-ERK^{+} non-CIN neurons reported as percent of total non-CIN neurons in the DM or DL
283 striatum. (n = 6-8 Striata per genotype; Two-way RM ANOVA; Post hoc Šídák's multiple
284 comparisons test: n.s. indicates p > 0.05). **(D)** Representative images of p-rpS6 and ChAT
285 expression in the DL striatum of Unlesioned (no 6-OHDA hemisphere + L-Dopa washout
286 condition) and Lesioned + L-Dopa conditions. White rectangle indicates inset image of p-rpS6
287 heat map displayed for a single CIN. **(E)** Quantification of normalized CIN p-rpS6 intensity in
288 the DL striatum of Unlesioned hemispheres (no 6-OHDA hemisphere + L-Dopa washout
289 condition). **(F)** Quantification of normalized CIN p-rpS6 intensity in the DL striatum of 6-
290 OHDA Lesioned hemispheres with and without L-Dopa washout (n = 150+ CIN from 12-16
291 Striata per genotype; ANOVA; Main effect: F [5, 1517] = 7.05, p <0.00001. Post hoc Tukey's
292 multiple comparisons test: **p < 0.01). **(G)** Plot of individual CIN p-rpS6 intensities across
293 relative distance from DL apex of the striatum. Best-fit lines for each condition are plotted.

294

Tables: None

Other Files: None

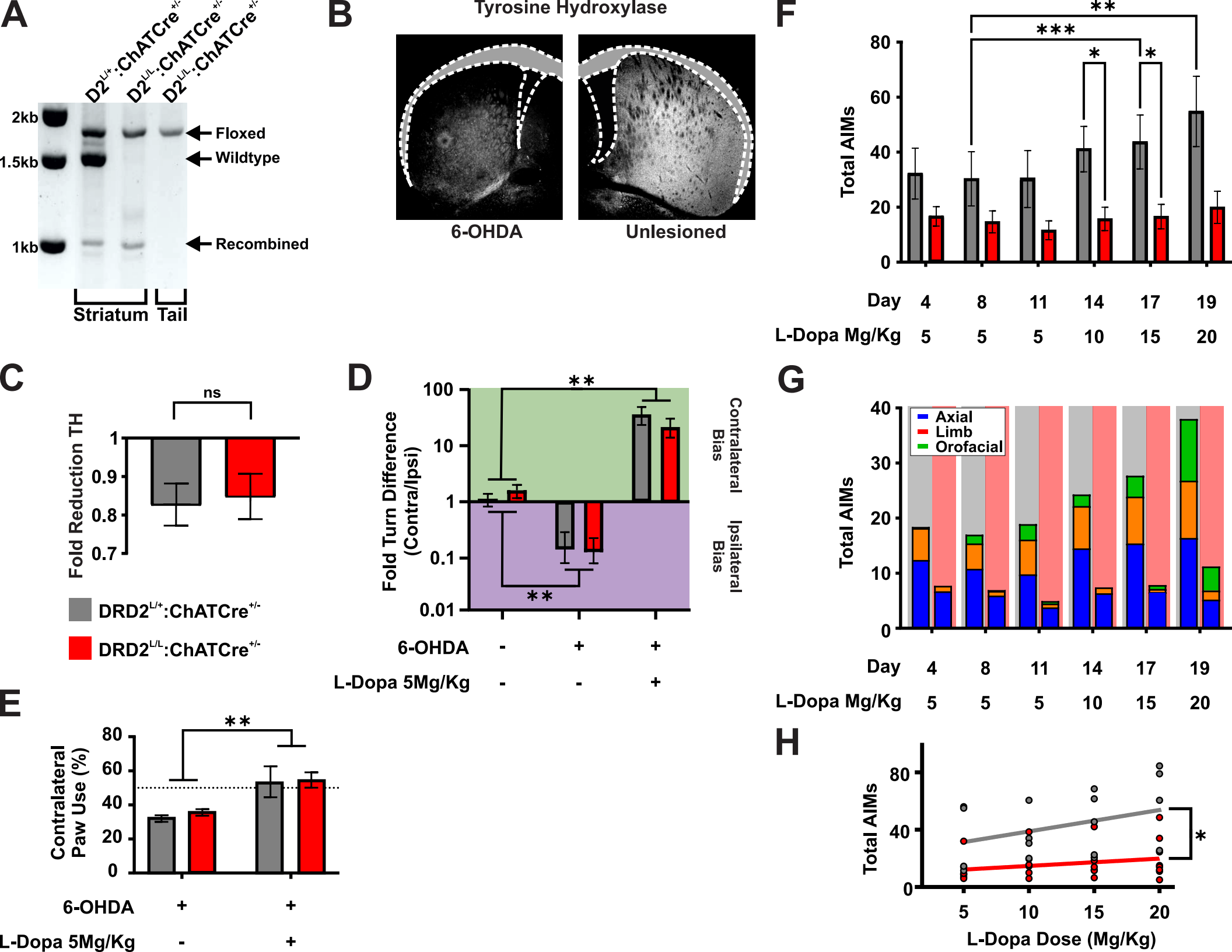
A
D2L/+:ChATCre+/-
D2L/L:ChATCre+/-
D2L/L:ChATCre+/-
2kb
1.5kb
1kb
Floxed
Wildtype
Recombined
Striatum
Tail
B
Tyrosine Hydroxylase
6-OHDA
Unlesioned
C
ns
Fold Reduction TH
1
0.9
0.8
0.7
DRD2L/+:ChATCre+/-
DRD2L/L:ChATCre+/-
D
**
100
10
1
0.1
0.01
Fold Turn Difference (Contra/Ipsi)
Contralateral Bias
Ipsilateral Bias
6-OHDA - + +
L-Dopa 5Mg/Kg - - +
E
**
Contralateral Paw Use (%)
80
60
40
20
0
6-OHDA + +
L-Dopa 5Mg/Kg - +
F
**
***
*
*
Total AIMs
80
60
40
20
0
Day 4 8 11 14 17 19
L-Dopa Mg/Kg 5 5 5 10 15 20
G
Axial
Limb
Orofacial
Total AIMs
40
30
20
10
0
Day 4 8 11 14 17 19
L-Dopa Mg/Kg 5 5 5 10 15 20
H
Total AIMs
80
40
0
*
5 10 15 20
L-Dopa Dose (Mg/Kg)

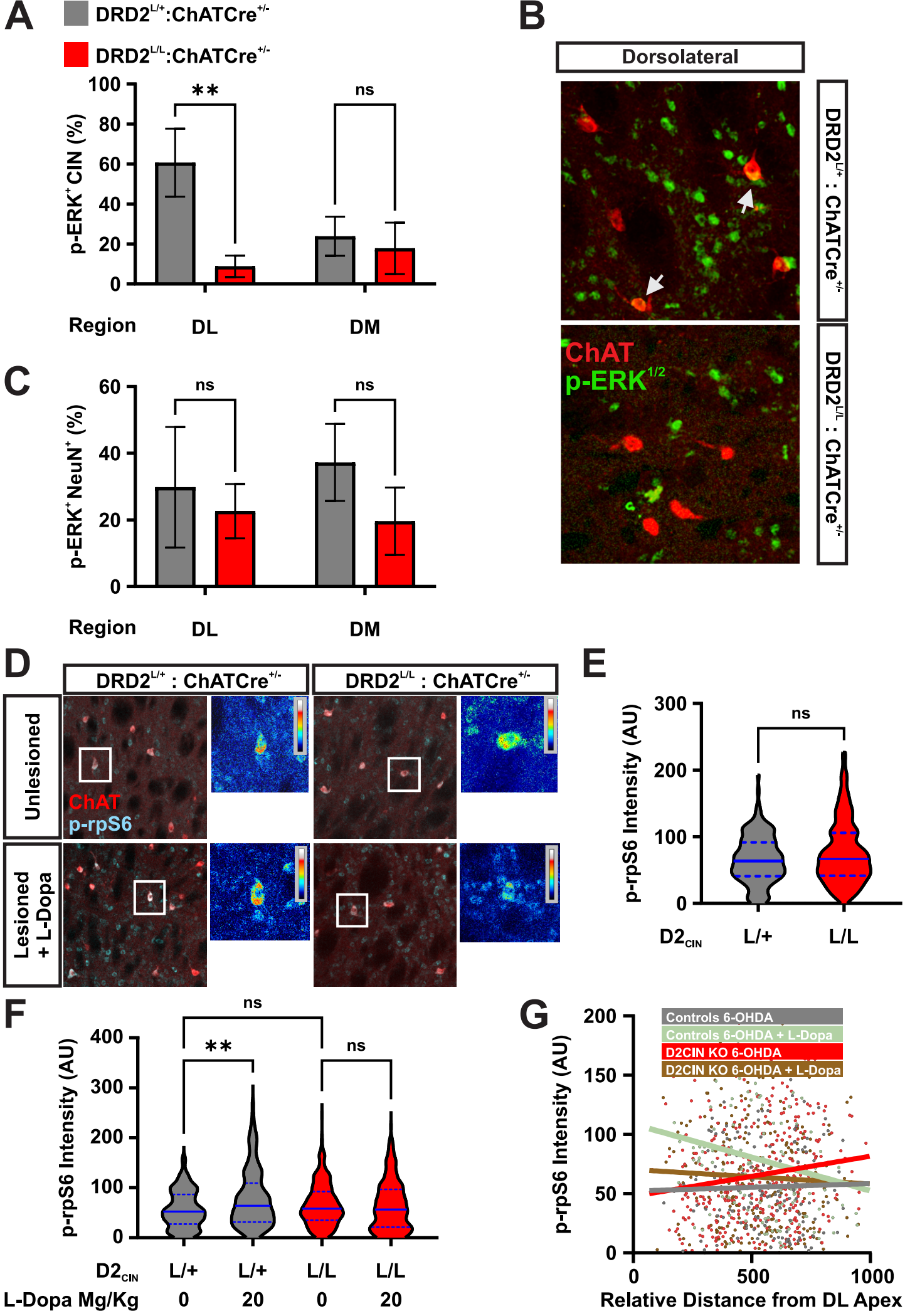
A
DRD2L/+:ChATCre+/-
DRD2L/L:ChATCre+/-
p-ERK+ CIN (%)
100
80
60
40
20
0
**
ns
Region
DL
DM
B
Dorsolateral
DRD2L/+ : ChATCre+/-
DRD2L/L : ChATCre+/-
ChAT
p-ERK1/2
C
p-ERK+ NeuN+ (%)
60
40
20
0
ns
ns
Region
DL
DM
D
DRD2L/+ : ChATCre+/-
DRD2L/L : ChATCre+/-
Unlesioned
Lesioned + L-Dopa
ChAT
p-rpS6
E
p-rpS6 Intensity (AU)
300
200
100
0
ns
D2CIN
L/+
L/L
F
p-rpS6 Intensity (AU)
400
300
200
100
0
ns
**
ns
D2CIN
L/+
L/+
L/L
L/L
L-Dopa Mg/Kg
0
20
0
20
G
Controls 6-OHDA
Controls 6-OHDA + L-Dopa
D2CIN KO 6-OHDA
D2CIN KO 6-OHDA + L-Dopa
p-rpS6 Intensity (AU)
200
150
100
50
0
0
500
1000
Relative Distance from DL Apex